An application of the Least Squares 3D algorithm for territorial monitoring and control

V. Barrile, G. M. Meduri, and G. Bilotta

Abstract— In this contribute we propose an application of a new algorithm for least squares matching of overlapping 3D surfaces that we sampled point by point using a terrestrial laser scanner. The studies on the absolute orientation of stereo models using DEMs as control information are known as DEM matching. The proposed method estimates the transformation parameters between two (or more) fully 3D surface patches and minimizes the Euclidean distances instead of Z-differences between the surfaces by least squares. The application in question is aimed, in the study of deformations of mountain areas, as well as test the TLS applied to a hilly area. For this purpose, it was also tested using the algorithm LS3D "Least squares 3D surface matching" that allows both the registration of point clouds produced by scans carried out without using targets but, overall, the estimate of deformations that in this case, compared to other methods, is done directly on the basis of the two data sets acquired in two different eras.

Keywords—Laser scanner 3D, Least squares 3D surface matching, Radiometric data, Survey.

I. INTRODUCTION AND STUDY AREA

THE Faculty of Agriculture of the University "Mediterranea" of Reggio Calabria is built on a hill that offers a specific geomorphology. In fact, after the construction of the Faculty building some problems arose, regarding its stability, the possible deformations through time also because of poor vegetation.
The Laboratory of Geomatics Engineering Faculty of the University "Mediterranea" of Reggio Calabria, used Terrestrial Laser Scanner for monitoring the hill, doing the scans after three years and examining the results obtained. Every era we made two scans, that we found to be sufficient to cover the entire study area.

In photogrammetry, the problem statement of surface patch matching and its solution method was first addressed by Gruen (1985a) as a straight application of Least Squares Matching.

The Least Squares Matching concept had been applied to many different types of measurement and feature extraction problems due to its high level of flexibility and its powerful mathematical model.

If 3D point clouds derived by any device or method represent an object surface, the problem should be defined as a surface matching problem instead of the 3D point cloud matching. This method, Least Squares 3D Surface Matching (LS3D), estimates the 3D transformation parameters between two or more fully 3D surface patches, minimizing the Euclidean distances between the surfaces by least squares.

An observation equation is written for each surface element on the template surface patch, i.e. for each sampled point. The geometric relationship between the conjugate surface patches is defined as a 7-parameter 3D similarity transformation. This parameter space can be extended or reduced, as the situation demands it. The constant term of the adjustment is given by the observation vector whose elements are Euclidean distances between the template and search surface elements.

Fig. 1 study area

Fig. 2 a view of the scanner

V. Barrile is with the DICEAM Department, Faculty of Engineering Mediterranean University of Reggio Calabria, Reggio Calabria 89100 IT (phone: +39-0965-875-301; e-mail: vincenzo.barrile@unirc.it).

G. M. Meduri is with the DICEAM Department, Faculty of Engineering Mediterranean University of Reggio Calabria, Reggio Calabria 89100 IT (e-mail: giumed@libero.it).

G. Bilotta was with the Department of Planning, IUAV University of Venice, Venice 30135 IT. She now collaborates with the DICEAM Department, Faculty of Engineering Mediterranean University of Reggio Calabria, Reggio Calabria 89100 IT (e-mail: giuliana.bilotta@gmail.com).

II.   REGISTRATION OF THE SCANS

The first operation performed after the relief phase was therefore recording different scans with a procedure based on the algorithm of "Least Squares 3D surface matching".
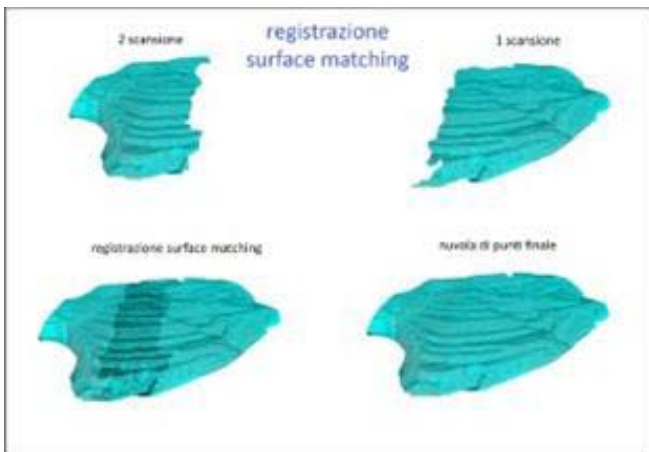

Fig. 3 some views of the scans

Fig. 4 Schematization of the surface matching with LS3D

Assume that two different surfaces of the same object are sampled point by point, at different times (temporally) or from different viewpoints (spatially). $f(x,y,z)$ and $g(x,y,z)$ are conjugate regions of the object in the left and right surfaces respectively.

The mathematical model used considers the reflection that, at every point of the first surface $f(x,y,z)$ has an exact match with $g(x,y,z)$.

The functional model is:

$$f(x,y,z)=g(x,y,z) \qquad (1)$$

According to Eq. (1) each surface element on the template surface patch $f(x,y,z)$ has an exact correspondent surface element on the search surface $g(x,y,z)$, or vice-versa, if both of the surfaces would analytically be continuous surfaces without any deterministic or stochastic discrepancies. In order to model the stochastic discrepancies, which are assumed to be random errors, and may stem from the sensor, environmental conditions or measurement method, a true error vector $e(x,y,z)$ is added as:

$$f(x,y,z)-e(x,y,z)=g(x,y,z) \qquad (2)$$

Eq. (2) are observation equations, which functionally relate the observations $f(x,y,z)$ to the parameters of $g(x,y,z)$. The matching is achieved by least squares minimization of a goal function, which represents the sum of squares of the Euclidean distances between the template and the search surface elements:

$$\sum \|d\|^2 = min \qquad (3)$$

and in Gauss form:

$$[dd]=min$$

where d stands for the Euclidean distance.

The final location is estimated with respect to an initial position of $g(x,y,z)$, the approximation of the conjugate search surface $g^0(x,y,z)$.

To express the geometric relationship between the conjugate surface patches, a 7-parameter 3D similarity transformation is used:

$$[x \ y \ z]^T = t + mRx_0 \qquad (4)$$

$$x=t_x+m(r_{11}x_0+r_{12}y_0+r_{13}z_o) \qquad (5)$$
$$y=t_y+m(r_{21}x_0+r_{22}y_0+r_{23}z_o)$$
$$z=t_z+m(r_{31}x_0+r_{32}y_0+r_{33}z_o)$$

where $r_{ij} = R(\omega,\varphi,\kappa)$ are the elements of the orthogonal rotation matrix, $[t_x \ t_y \ t_z]^T$ is the translation vector, and m is the central dilation.

In order to perform least squares estimation, Equation (2) must be linearized by Taylor expansion, ignoring 2nd and higher order terms.

$$f(x,y,z,)-$$
$$e(x,y,z)=g^0(x,y,z)+\frac{\partial g^0(x,y,z)}{\partial x}dx+\frac{\partial g^0(x,y,z)}{\partial y}dy+\frac{\partial g^0(x,y,z)}{\partial z}dz \quad (6)$$

with

$$dx=\frac{\partial x}{\partial p_i}dp_i \quad , \quad dy=\frac{\partial y}{\partial p_i}dp_i \quad , \quad dz=\frac{\partial z}{\partial p_i}dp_i \qquad (7)$$

where $p_i \in \{t_x,t_y,t_z,m,\omega,\varphi,\kappa\}$ is the i-th transformation parameter in Eq. (5). Differentiation of Eq. (5) gives:

$$dx=dt_x+a_{10}dm+a_{11}d\omega+a_{12}d\varphi+a_{13}d\kappa \qquad (8)$$
$$dy=dt_y+a_{20}dm+a_{21}d\omega+a_{22}d\varphi+a_{23}d\kappa$$
$$dz=dt_z+a_{30}dm+a_{31}d\omega+a_{32}d\varphi+a_{33}d\kappa$$

where a_{ij} are the coefficient terms, whose expansion are trivial. Using the following notation

$$g_x = \frac{\partial g^o(x,y,z)}{\partial x} \quad , \quad g_y = \frac{\partial g^o(x,y,z)}{\partial y} \quad , \quad g_z = \frac{\partial g^o(x,y,z)}{\partial z} \quad (9)$$

and substituting Eq. (8), Eq. (6) results in the following:

$$-e(x,y,z) = g_x dt_x + g_y dt_y + g_z dt_z + \quad (10)$$
$$+ (g_x a_{10} + g_y a_{20} + g_z a_{30}) dm + (g_x a_{11} + g_y a_{21} + g_z a_{31}) d\omega +$$
$$+ (g_x a_{12} + g_y a_{22} + g_z a_{32}) d\varphi + (g_x a_{13} + g_y a_{23} + g_z a_{33}) d\kappa - (f(x,y,z) -$$
$$+ g^0(x,y,z)).$$

Fig. 5 global cloud of points cleaned after the recording with LS3D of the scan at the time t_1

Fig. 6 global cloud of points cleaned after the recording with LS3D of the scan at the time t_2

In the context of the Gauss–Markoff model, each observation is related to a linear combination of the parameters, which are variables of a deterministic unknown function that constitutes the functional model of the whole mathematical model.

The terms $\{g_x, g_y, g_z\}$ are numeric 1st derivatives of this function $g(x,y,z)$.

Eq. (10) gives in matrix notation

$$-e = Ax - l \,, \, P \quad (11)$$

where A is the design matrix, $x^T = [dt_x \, dt_y \, dt_z \, dm \, d\omega \, d\varphi \, d\kappa]$ is the parameter vector, and $l = f(x,y,z) - g^0(x,y,z)$ is the constant vector that consists of the Euclidean distances between the template and correspondent search surface elements.

In our implementation the template surface elements are approximated by the data points.

In general, both surfaces (template and search) can be represented in any kind of piecewise form.

With the statistical expectation operator E{} and the assumptions

$$e \sim N(0, \sigma_0^2 Q_{ll)} \,, \, \sigma_0^2 Q_{ll} = \sigma_0^2 P_{ll}^{-1} = K_{ll} = E\{ee^T\} \quad (12)$$

the system (11) and (12) is a Gauss–Markoff estimation model. Qll, $P = Pll$ and Kll stand for a priori cofactor, weight and covariance matrices respectively.

The unknown transformation parameters are treated as stochastic quantities using proper weights. This extension gives advantages of control over the estimating parameters [7].

In the case of poor initial approximations for unknowns or badly distributed 3D points along the principal component axes of the surface, some of the unknowns, especially the scale factor m, may converge to a wrong solution, even if the scale factors between the surface patches are same. We introduce the additional observation equations regarding the system parameters as

$$-e_b = Ix - l_b \,, \, P_b \quad (13)$$

where I is the identity matrix, lb is the (fictitious) observation vector for the system parameters, and Pb is the associated weight coefficient matrix. The weight matrix Pb has to be chosen appropriately, considering a priori information of the parameters. An infinite weight value $((Pb)ii \rightarrow \infty)$ excludes the i-th parameter from the system assigning it as constant, whereas zero weight $((Pb)ii = 0)$ allows the i-th parameter to vary freely assigning it as unknown parameter in the classical meaning.

The least squares solution of the joint system Eqs. (11) and (13) gives as the Generalized Gauss–Markoff model the unbiased minimum variance estimation for the parameters

$$x\square = (A^T PA + P_b)^{-1}(A^T Pl + P_b l_b) \text{ solution vector} \quad (14)$$

$$\sigma\square_o = \frac{v^T Pv + v_b^T P_b v_b}{r} \quad \text{variance factor} \quad (15)$$

$$v = Ax\square - l \quad \text{residual vector for surface observation} \quad (16)$$

$$v_b = Ix\square - l_b \quad \text{residual vector for parameter observation} \quad (17)$$

where ˆ stands for the Least Squares Estimator, r = n-u is the redundancy, n is the number of observations that is equivalent to the number of elements of the template surface, and u is the number of transformation parameters that is seven here. When the system converges, the solution vector converges to zero $(x\square \rightarrow 0)$. Then the residuals of the surface observations vi become the final Euclidean distances between the estimated search surface and the template surface patches.

$$v_i = g\square(x,y,z)_i - f(x,y,z)_i \,, \, i\{1,\ldots,n\}. \quad (18)$$

The function values $g(x,y,z)$ in Eq. (2) are actually stochastic quantities. This fact is neglected here to allow for

the use of the Gauss–Markoff model and to avoid unnecessary complications, as typically done in LSM [6].

This assumption is valid and the omissions are not significant as long as the random errors of the template and search surfaces are normally distributed and uncorrelated. In the extreme case when the random errors of both surfaces show systematic and dependency patterns, which is most probably caused by defect or imperfectness of the measurement technique or the sensor, it should be an interesting study to investigate the error behaviour using the Total Least Squares (TLS) method [3]. The TLS is a relatively new adjustment method of estimating parameters in linear models that include errors in all variables [10].

The functional model is non-linear. The solution iteratively approaches a global minimum. With the solution of linearized functional models there is always a danger to find local minima. A global minimum can only be guaranteed if the function is expanded to Taylor series at such a point where the approximate values of the parameters are close enough to their true values ($p_i^0 \cong p_i \in \mathbb{R}^u, i = 1, \ldots, u$) in parameter space. We ensure this condition by providing of good quality initial approximations for the parameters in the first iteration:

$$p_i^0 \in \{t_x^0, t_y^0, t_z^0, m^0, \omega^0, \varphi^0, \kappa^0\}$$ (19)

After the solution vector (14) has been solved for, the search surface is deformed to a new state using the updated set of transformation parameters, and the design matrix A and the constant vector l are reevaluated.

The iteration stops if each element of the alteration vector x in Eq. (14) falls below a certain limit:

$$|dp_i| < c_i,$$
$$dp_i \in \{dt_x, dt_y, dt_z, dm, d\omega, d\varphi, d\kappa\}$$ (20)

where $i=\{1,2,\ldots,7\}$.

Adopting the parameters as stochastic variables allows adapting the dimension of the parameter space in a problem-specific manner. In the case of insufficient a priori information on the geometric deformation characteristics of the template and search surfaces, the adjustment could be started employing a high order transformation, e.g. 3D affine. However, this approach very often leads to an over-parameterization problem.

Therefore, during the iterations an appropriate test procedure that is capable to exclude non-determinable parameters from the system should be performed.

The terms {gx , gy , gz} are numeric derivatives of the unknown surface patch g(x,y,z). Its calculation depends on the analytical representation of the surface elements. As a first method, let us represent the search surface elements as plane surface patches, which are constituted by fitting a plane to 3 neighboring knot points, in the implicit form:

$$g^0(x, y, z) = Ax + By + Cz + D = 0$$ (21)

where A, B, C, and D are parameters of the plane. Using the mathematical definition of the derivation, the numeric 1st derivation according to the x-axis is

$$g_x = \frac{\partial g^0}{\partial x} = \lim_{\Delta x \to 0} \frac{g^0(x,y,z) - g^0(x,y,z)}{\Delta x}$$ (22)

where the numerator term of the equation is simply the distance between the plane and the off-plane point (x+Δx,y,z). Then using the point-to-plane distance formula,

$$g_x = \frac{A(x+\Delta x) + By + Cz + D}{\Delta x \sqrt{A^2 + B^2 + C^2}} = \frac{A}{\sqrt{A^2 + B^2 + C^2}}$$ (23)

is obtained. Similarly gy and gz are calculated numerically.

$$g_y = \frac{B}{\sqrt{A^2 + B^2 + C^2}},$$
$$g_z = \frac{A}{\sqrt{A^2 + B^2 + C^2}}$$ (24)

Actually these numeric derivative values {gx , gy , gz} are x-y-z components of the local surface normal vector at that point.

$$\vec{n} = \frac{\vec{\nabla}g^0}{\|\vec{\nabla}g^0\|} = \frac{\left[\frac{\partial g^0}{\partial x} \frac{\partial g^0}{\partial y} \frac{\partial g^0}{\partial z}\right]^T}{\|\vec{\nabla}g^0\|} = \frac{[A \; B \; C]^T}{\sqrt{A^2 + B^2 + C^2}}$$ (25)

In the case of representation of search surface elements as parametric bi-linear surface patches, which are constituted by fitting the bi-linear surface to 4 neighboring knot points $P_{i,j}$:

$$\vec{G}(u,w) = \overrightarrow{P_{0,0}}(1-u)(1-w) + \overrightarrow{P_{0,1}}(1-u)w + \overrightarrow{P_{0,1}}u(1-w) + \overrightarrow{P_{1,1}}uw$$ (26)

where u,w $\in [0,1]^2$ and G, Pi,j $\in \mathcal{R}^3$. Again the numeric derivative terms {gx , gy , gz} are calculated from components of the local surface normal vector on the parametric bi-linear surface patch:

$$\vec{n} = [g_x g_y g_z]^T = \frac{\vec{\nabla}G}{\|\vec{\nabla}G\|} = \frac{\frac{\partial \vec{G}(u,w)}{\partial u} \times \frac{\partial \vec{G}(u,w)}{\partial w}}{\|\vec{\nabla}G\|}$$ (27)

With this approach a better a posteriori sigma value could be obtained due to a smoothing effect. In the case of insufficient initial approximations, the numeric derivatives {gx, gy , gz} can be calculated on the template surface patch f(x,y,z) instead of on the search surface g(x,y,z) in order to speed-up the convergence.

TABLE I - Numerical results of the "surface matching" LS3D with the two clouds of point at the time t_1

No	TMP scan no (#)	SRC scan no (#)	No.of TMP points (K)	No.of SRC points (K)	No. of COR points (K)	Inter.	Time (sec)	Sigma naught (cm)
1	1	2	2063	2008	1376	3	1324	0,3

TABLE II - Numerical results of the "surface matching" LS3D with the two clouds of point at the time t_2

No	TMP scan no (#)	SRC scan no (#)	No.of TMP points (K)	No.of SRC points (K)	No. of COR points (K)	Inter.	Time (sec)	Sigma naught (cm)
1	1	2	1978	2043	1412	3	1342	0,3

The matching for the registration of the whole cloud at the epochs t1 and t2 presupposes the selection of three points in common on the scans to be joined; by applying the matching several times using different homologous points, the results were validated using the statistical test χ^2.

The variable χ2 measures the overall difference between observed and expected data according expression:

$$\chi^2 = \sum_{i=1}^{N} \frac{(f_{0i} - f_{Ai})^2}{f_{Ai}}$$

The test $\chi^2(p_1, \alpha) < \chi^2 < \chi^2(p_2, \alpha)$ for a risk error α equal to 5% is verified result.

III. SUBSEQUENT PROCESSING - CONTROL OF DEFORMATION

Once registered scans for the generation of clouds at two times t_1 and t_2, the "global matching" is re-applied to monitor the deformation.

The procedure involves three steps:
- global matching of the two point clouds over the area selected as stable;
- global matching of all points of the clouds over an area already found stable and searching for areas of possible movement;
- local matching of selected areas to estimate the deformation.

In the first step the algorithm LS3D is applied to areas that we assume as stable, eliminating areas with possible movements; the two clouds (registered) at the two epochs are traced thus in a common reference system.

Fig. 7 stable area chosen for the global "matching"

TABLE III - Numerical results of the "global matching" of the clouds of point at the time t_1 and t_2

No	TMP scan no (#)	SRC scan no (#)	No.of TMP points (K)	No.of SRC points (K)	No. of COR points (K)	Inter.	Time (sec)	Sigma naught (cm)
1	1	2	487	486	486	2	303	0,3

The second step is based on the same matching technique, but drawing the two point clouds, already traced in the same reference system, and considering whole clouds, therefore not only stable areas but also the areas with possible movements.

TABLE IV- Global matching" considering the stable areas and those with possible movements

No	TMP scan no (#)	SRC scan no (#)	No.of TMP points (K)	No.of SRC points (K)	No. of COR points (K)	Inter.	Time (sec)	Sigma naught (cm)
1	1	2	2695	2609	2543	3	1793	0,25

To improve the reliability of the results obtained have been made more cycles of local "matching" and validating the results obtained through statistical tests.

The value of the Student's t test is calculated as the ratio of the observed mean difference and its standard error:

$$t = \bar{d} \sqrt{S_d^2/n}$$

where:

$$\bar{d} = \sum d_i/n$$ with d_i difference between the pairs of results obtained

$$S_d^2 = \sum (d_i - d)^2/(n-1)$$

The last stage of the method consists in the estimation of relative movement to some portions of the hill using the same method but using LS3D local matches in a "local matching".

Selected portions for analysis for each "patch" on the cloud at the time t_1 is automatically detected by the subset corresponding LS3D the cloud at the time t_2, thus obtaining

the seven transformation parameters that describe the deformation and in particular the three translations and the three rotations.

TABLE V - Results of monitoring of deformations of the two regions examined with LS3D (shifts measured in centimeters and rotations in gons (1 circle 400gons)

Deformation parameters	Unit	Cockpit	Rock
t_x	cm	0,11	0,32
t_y	cm	0,32	0,29
t_z	cm	-0,26	-0,52
ω	gon	0,2	0,1
φ	gon	0,1	0,05
k	gon	0,09	0,07
m	Pure number	1	1

Fig. 8 the areas chosen for the control of the deformations
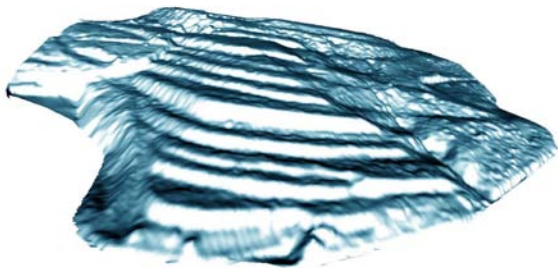

Fig. 9 3D model of the cloud of points

The results obtained with the LS3D are shown in the figure where various models are represented with the aid of the cloud of points.

Fig. 10 3D model of the cloud of points

Fig. 11 texture of the model

IV. VALIDATION RESULTS

The validation was based on the comparison of the six parameters estimated from the topographic data with those coming from the proposed TLS approach.

The points measured by total station have a standard deviation, estimated through repeated measurements, of about 1 mm in the depth direction Y, and of about 3 mm in the horizontal and vertical directions. Using 15-20 points to estimate the 6 transformation parameters of each panel the estimated standard deviation is below 1 mm for the translations, and below 0.1 gons for the rotations.

Therefore, for the purpose of this validation experiment, the topographic estimates can be used as the reference values, and the differences between the TLS estimates and those coming from topography directly represent the TLS errors.

As can be observed, the differences between two techniques are in most of the cases below one centimeter. Taking into account the non optimal characteristics of the used targets, from the point of view of the LS3D, these are promising results.

Fig. 12 spherical target in polystyrene 12 cm

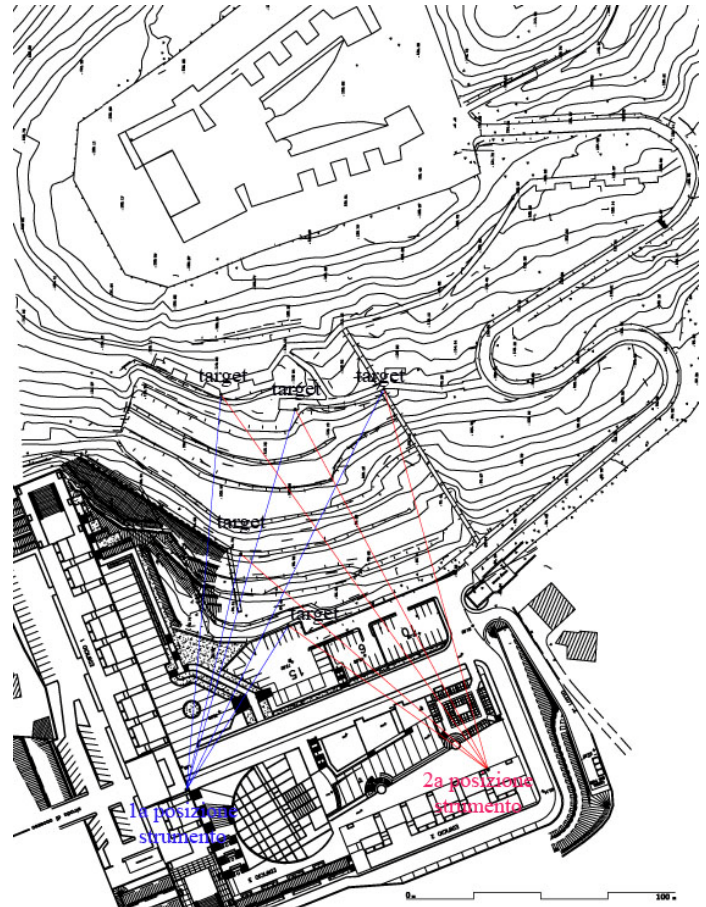Fig. 13 monumentation of the target

Fig. 14 map of the area with views of the positions of the instrument and the targets

V. CONCLUSION

Thanks to the obtained results we can say that the real deformation is almost zero. This is probable due to that the observed period coincides with the dry season, where the landslide is inactive. However there is no reason for expecting a degradation of the accuracy having bigger deformations. The experience carried out has highlighted the benefits of LS3D than other methods. The first is to exploit all the information provided by the geometry of the 3D cloud of points to be able to measure strain with a magnitude less than the accuracy of the instrument. The second is to implement a flexible procedure that can be applied with any type of scenes including a wide range of applications of deformation. The third is to measure movement in three dimensions, not only along a preferred direction.

REFERENCES

[1] P.J. Besl, N.D. McKay, "A method for registration of 3-D shapes", *IEEE Transactions on Pattern Analysis and Machine Intelligence*, vol. 14, issue 2, 1992, pp. 239-256.

[2] B. Crippa, "Computational algorithms and optimal procedures for the digital terrain models production", *Bollettino di Geodesia e Scienze Affini*, vol.1, 1991 ,pp.11-30.

[3] G.H. Golub, C.F. Van Loan, "An analysis of total least squares problem", *SIAM. J. Numer. Anal.*, Vol. 17, 1980, pp. 883-893.

[4] J. Gomes Mota, "Localisation of Mobile Robots using Scanned Laser and Reconstructed 3D Models", MSc Thesis, Instituto Superior Técnico, Universidade Técnica de Lisboa, Portugal, May 2002.

[5] S.J. Gordon, D.D. Lichti, "Terrestrial laser scanners with a narrow field of view: the effect on 3D resection solutions", *Survey Review*, vol. 37, issue 292, 2004, pp. 448-468.

[6] A. Gruen, "Adaptive least squares correlation: a powerful image matching technique", *South African Journal of Photogrammetry, Remote Sensing and Cartography*, vol. 14, 1985, pp. 175-187.

[7] A. Gruen, "Photogrammetrische Punktbestimmung mit der Buendelmethode", IGP ETH-Zürich, Mitt. Nr.40,1986, pp. 1-87.

[8]   A. Gruen, A. Devrim, "Least squares 3D surface and curve matching", *ISPRS Journal of Photogrammetry and Remote Sensing*, vol. 59, issue 3, 2005, pp. 151-174.

[9]   O. Monserrat, M. Crosetto, "Deformation measurement using terrestrial laser scanning data and least squares 3D surface matching", *ISPRS Journal of Photogrammetry and Remote Sensing*, vol. 63, issue 1, January 2008, pp. 142-154.

[10] B. Shaffrin, A.Y. Felus, "On total least-squares adjustment with constrains", *A Window on the Future of Geodesy: Proceedings of the XXIII General Assembly of the International Union of Geodesy and Geophysics,* Sapporo, 2003, pp.417-421.

[11] 4DiXplorer AG LS3D *User guide*.